Exact transfer-matrix enumeration and critical behaviour of self-avoiding walks across finite strips

1994 J. Phys. A: Math. Gen. 27 4055

(http://iopscience.iop.org/0305-4470/27/12/014)

J. Phys. A: Math. Gen. 27 (1994) 4055–4067. Printed in the UK

Exact transfer-matrix enumeration and critical behaviour of self-avoiding walks across finite strips

M T Batchelor and C M Yung

Mathematics Department, School of Mathematical Sciences, Australian National University, Canberra ACT 0200, Australia

Received 15 November 1993

Abstract. We use a transfer matrix with suitably defined vertex weights to algebraically enumerate n-step self-avoiding walks confined to cross an $L \times M$ rectangle on the square lattice. We construct the exact generating functions for self-avoiding walks from the south-west to south-east corners for $L = 1, 2, 3, 4, 5$ and infinite height M corresponding to a half-strip. We also consider the number of n-sided polygons rooted to the south-west corner of the half-strip and give a formulation to treat self-avoiding walks across the full strip. In each case, the exact generating functions are ratios of polynomials in the step fugacity. We investigate the singularity structure of the generating functions along with the finite-size scaling in M of the singularity in the analogue of the heat capacity. We find the critical exponents $\gamma = 1$ and $\gamma = 2$ for the half- and open strip, along with $\nu = \frac{1}{2}$. These results are indicative of the one-dimensional or Gaussian nature of self-avoiding walks in infinitely long, but finitely wide strips.

1. Introduction

Self-avoiding walks have been studied widely as models of macromolecular chains. The configurational properties of both free and confined chains are of particular interest. In recent papers, self-avoiding walks, confined to traverse an $L \times L$ square lattice, have been studied via a variety of techniques including exact enumeration [1], the transfer-matrix approach [2] and the renormalization group [3]. Exact values for the number $c_n(L)$ of n-step self-avoiding walks from the south-west (SW) to the north-east (NE) corner of the square have been enumerated for $L \leqslant 6$ [1]. As the system is finite, there is no phase transition. Nevertheless, the mean number of steps plays the role of an energy and there is a sharp peak in the analogue of the heat capacity. In terms of the chain generating function

$$C_L(x) = \sum_n c_n(L) x^n \tag{1.1}$$

this quantity is defined as [1]

$$V(x, L) = \langle n^2(x, L)\rangle - \langle n(x, L)\rangle^2 \tag{1.2}$$

where

$$C_L(x)\langle n(x, L)\rangle = x\frac{\mathrm{d}}{\mathrm{d}x}C_L(x) \tag{1.3a}$$

$$C_L(x)\langle n^2(x, L)\rangle = x\frac{\mathrm{d}}{\mathrm{d}x}\left[x\frac{\mathrm{d}}{\mathrm{d}x}C_L(x)\right]. \tag{1.3b}$$

It follows from standard finite-size scaling [2,4] that the value $x_{\mathrm{m}}(L)$ that maximizes $V(x, L)$ obeys

$$x_{\mathrm{m}}(L) - x_{\mathrm{c}} \sim L^{-1/\nu} \tag{1.4}$$

for large L. Here $x_{\mathrm{c}} = 0.379\ldots$ is the critical (bulk) value [5] and the exponent $\nu = \frac{3}{4}$ [6].

On the other hand, the generating function for unconfined self-avoiding walks diverges as

$$C(x) \sim A(x - x_{\mathrm{c}})^{-\gamma} \tag{1.5}$$

where the amplitude A is a constant and the exponent $\gamma = \frac{43}{32}$ [6]. It follows that the number of n-step walks diverges as

$$c_n \sim B\mu^n n^{\gamma-1} \tag{1.6}$$

for large n where B is constant. The connective constant for self-avoiding walks follows as $\mu = 1/x_{\mathrm{c}}$.

Returning to confined walks, the total number of self-avoiding walks from corner to corner, following from (1.1) as $C_L(1)$, was extended to $L \leqslant 9$ by the transfer-matrix technique [2]. Subsequently, one of us considered the analogous problem for self-avoiding walks crossing an $L \times M$ rectangle [7]. There it was shown that the total number of walks to height M obeyed a linear recurrence relation whose depth increased rapidly with the width L. These recurrence relations were obtained explicitly on the square lattice for strip widths up to $L = 4$. Previous exact results for the largest eigenvalue of the transfer matrix for $L = 1$ and $L = 2$ [8,9] were thus extended, as the largest real root of the recurrence relation coincided with the maximum eigenvalue of the transfer matrix [7].

In this paper, we consider self-avoiding walks confined to an $L \times M$ rectangle and use a transfer matrix with suitably defined vertex weights to *algebraically* construct the generating function using MATHEMATICA. In this way, for example, we are able to reproduce the square $L = 6$ enumeration results [1] in 30 min on a workstation. The advantage of the transfer-matrix approach in the present geometry is that the exact enumeration is achieved via matrix multiplication, thus providing the complete generating function for large values of M, for given L, with relative ease.

The content and arrangement of the paper is as follows. In section 2, we discuss our construction of the self-avoiding-walk transfer matrix. We then apply it to walks from the SW to the SE corners, confined to the $L \times M$ rectangle, and construct the exact generating functions for *infinite* M for $L = 1, 2, 3, 4, 5$. The singularity structure for finite L is then investigated along with the finite-size scaling in M of the singularity in the analogue of the heat capacity. We then give a formulation to count the number of n-step self-avoiding walks from one side of an infinitely long strip to the other. Explicit generating functions are also constructed for this case. Finally, in section 3 we derive generating functions for the number of self-avoiding polygons rooted to the SW corner of an infinitely long rectangle. A discussion of the results is given in section 4.

2. Self-avoiding walks

We begin with the $L \times M$ rectangle, depicted in figure 1, with $\ell = L + 1$ columns and $m = M + 1$ rows.

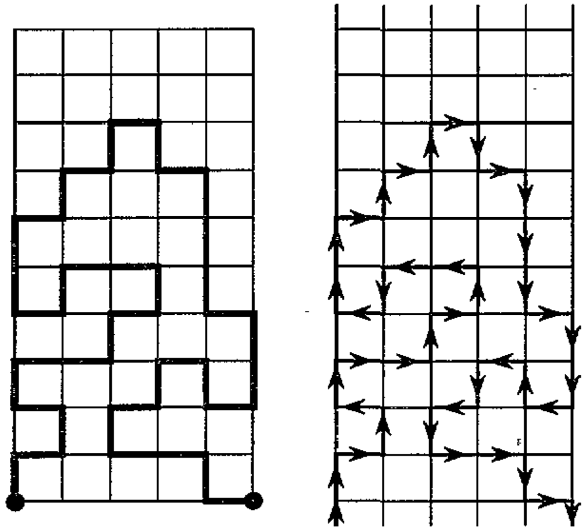

(*a*) (*b*)

Figure 1. (*a*) A typical self-avoiding walk on the square lattice between the SW and SE corners of a finite $L \times M$ rectangle. Here, $L = 5$ and $M = 10$. (*b*) The same walk as an arrow configuration in the half-strip.

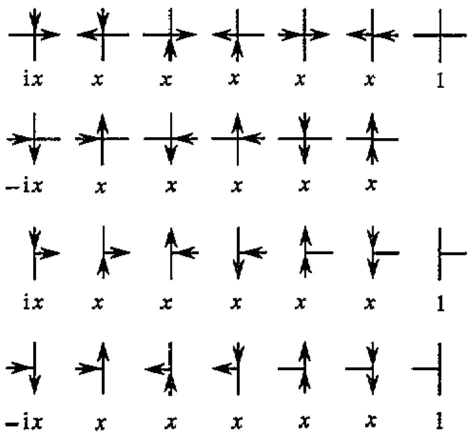

Figure 2. The allowed arrow configurations and corresponding vertex weights for self-avoiding walks on a strip of the square lattice. The variable x is the step fugacity.

2.1. Construction of the transfer matrix

To enumerate self-avoiding walks across the strip, we define a $3^\ell \times 3^\ell$ local transfer matrix $\mathbf{T}$ acting between adjacent rows of the lattice. Explicitly, we write

$$\mathbf{T} = \prod \text{vertex weights} \tag{2.1}$$

where the 13 bulk and 14 boundary vertex weights and their corresponding arrow configurations are given in figure 2. These weights reduce to those used in [7] when

Table 1. Values of $c_n(5, M)$. The values for $M = 10$ correspond to n-step self-avoiding walks from the SW to the SE corner of the rectangle of figure 1(a).

n	$M = 5$	$M = 10$
5	1	1
7	15	15
9	85	85
11	335	335
13	1237	1237
15	4638	4638
17	15 860	17 680
19	44 365	68 457
21	99 815	268 436
23	181 995	1 061 505
25	262 414	4 216 349
27	285 086	16 757 645
29	218 011	66 060 680
31	104 879	252 376 882
33	26 344	899 142 725
35	1770	2 868 674 184
37		7 991 872 363
39		19 265 137 388
41		40 146 355 170
43		72 366 003 717
45		112 694 212 921
47		150 923 309 039
49		172 262 775 891
51		165 082 511 222
53		129 719 062 830
55		80 572 023 472
57		37 424 893 398
59		12 006 207 870
61		2 403 974 376
63		257 492 990
65		11 341 696

$x = 1$. Unlike the corresponding vertex model on the honeycomb lattice, which is exactly solvable [10], we have no reason to believe that the present model is exactly solvable.

Note that our construction of the transfer matrix differs from those given previously for self-avoiding walks [9, 11] (see also [12]). Our transfer matrix is directly related to the O(n) models of Nienhuis [13, 6, 14] where the self-avoiding constraint is implicitly taken care of by the zero fugacity of each closed loop ($n = \mathrm{i} - \mathrm{i} = 0$)—*à la* de Gennes [15].

2.2. Generating functions for the half-strip

The generating function for self-avoiding walks from the SW to the SE corner of the $L \times M$ rectangle is given by

$$C_{L,M}(x) = \sum_n c_n(L, M)x^n \tag{2.2}$$

or, in terms of the transfer matrix,

$$C_{L,M}(x) = \langle\phi|\mathbf{T}^m|\psi\rangle/(-\mathrm{i}x) \tag{2.3}$$

with the initial and final states $\phi = \uparrow \| \cdots \| \downarrow$ and $\psi = |\| \cdots \||$, respectively. Note that we need to divide the matrix element by $-\mathrm{i}x$ to compensate for the weight of the overall half-loop and the initial and final bonds.

For a given value of L, we have constructed the above transfer matrix algebraically using MATHEMATICA and then obtained the generating function $C_{L,M}(x)$ for given M via (2.3). We have particularly chosen the walk from the SW to the SE corner because the coefficients $c_n(L, M)$ appearing in the generating function, which define the number of allowed n-step walks, become fixed with increasing M. For such walks, the minimum number of steps is given by $n_{\min} = L$, whilst $n_{\max} = LM + L$ if L is even and $n_{\max} = (L+1)M + L$ if L is odd. For later reference, the exact values of $c_n(5, M)$ are given in table 1 for $M = 5$ and $M = 10$.

We are able to derive the generating function for as large a value of M as desired, subject to computer memory and time constraints. Naturally, it is desirable to sum the series and thus present the generating function in closed form. We have found that this is indeed possible in the $M \to \infty$ limit. This is due to the rational nature of the generating function and constitutes our major finding. The generating functions are of the general form

$$C_{L,\infty}(x) = \frac{p_L(x)}{q_L(x)}. \tag{2.4}$$

Our evidence for this is from a Padé analysis of the series, again using MATHEMATICA.

If the generating function is rational, the Padé approximants $P[N/N]$ and $Q[N/N]$, for large enough N (for instance), should converge to the exact numerator and denominator given a long enough series.

Defining $y = x^2$, our results for the polynomials $p_L(x)$ and $q_L(x)$ appearing in (2.4) are:

$$\begin{aligned}
p_1(x) &= x \\
q_1(x) &= 1 - y \\
p_2(x) &= y(1+y) \\
q_2(x) &= (1+y^2)(1-2y) \\
p_3(x) &= xy(1-y)(1+y)^2(1+y-5y^2+2y^3) \\
q_3(x) &= 1 - 4y + 3y^2 + 2y^3 - 4y^4 + 2y^5 - y^6 + 8y^7 - 5y^8 - 2y^9 + 4y^{10} \\
p_4(x) &= y^2(1+y)(1+3y-15y^2-8y^3+58y^4-29y^5-109y^6+198y^7+25y^8-335y^9+260y^{10} \\
&\quad +174y^{11}-414y^{12}+85y^{13}+338y^{14}-286y^{15}-70y^{16}+231y^{17}-132y^{18}-2y^{19} \\
&\quad +36y^{20}-23y^{21}+6y^{22}) \\
q_4(x) &= 1-6y+8y^2+12y^3-40y^4+15y^5+71y^6-133y^7+76y^8+132y^9-182y^{10}-43y^{11} \\
&\quad +390y^{12}-270y^{13}-379y^{14}+672y^{15}-51y^{16}-714y^{17}+535y^{18}+402y^{19} \\
&\quad -871y^{20}+264y^{21}+351y^{22}-324y^{23}+33y^{24}+39y^{25}-4y^{27}.
\end{aligned} \tag{2.5}$$

The results for $L = 5$ are listed in the appendix. In this case, we needed to generate terms greater than $O(x^{333})$ for which $c_{333}(5, \infty) = 689\,748\,737\,066\,148\,255\,207\,491\,121\,477\,693\,131\,872\,595\,709\,902\,690\,238\,279\,536\,921\,638\,845\,521\,002\,925\,162\,579\,919\,466\,390\,032\,106$. The complete construction of the $L = 5$ generating function took ~ 36 h on a workstation.

2.2.1. Recurrence relations. We have observed that a linear recurrence relation exists among the series coefficients $c_n(L,\infty)$. Such a recurrence relation is to be expected given the rational form (2.4) of the generating function. Writing the pole function $q_L(x)$ as

$$q_L(x) = \sum_{i=0}^{\mathcal{D}} a_i\, y^i \tag{2.6}$$

where $a_0 = 1$, the recurrence relation is

$$c_n(L,\infty) = -\sum_{i=1}^{\mathcal{D}} a_i c_{n-i}(L,\infty). \tag{2.7}$$

Thus the depth $\mathcal{D}$ of the recurrence relation is given by the degree of the polynomial $q_L(x)$ in y. Moreover, this implies a reciprocal relation between the zeros of $q_L(x)$ and the roots of the recurrence relation, as the latter are defined by the characteristic equation

$$\sum_{i=0}^{\mathcal{D}} a_i \lambda^{\mathcal{D}-i} = 0. \tag{2.8}$$

For each of the cases we have explicitly constructed, the zeros of $q_L(x)$ are all distinct, i.e. the recurrence relations amongst the $c_n(L,\infty)$ involve no multiple roots.

We now turn to the critical behaviour.

2.2.2. Singularity structure for finite L. The poles of $C_{L,\infty}(x)$, i.e. the zeros of $q_L(x)$, are shown in figure 3 for $L = 2, 3, 4, 5$. The exact value $x_c(L)$ of the dominant pole is given in table 2 as a function of increasing L. Also shown are the approximate values obtained via Padé approximants for $L = 6$ and $L = 7$ from shorter series. It is clear that the values are tending towards the bulk value $x_c = 0.379\ldots$ as L increases. The generating function behaves as

$$C_{L,\infty}(x) \sim A_L (x - x_c(L))^{-1}. \tag{2.9}$$

Thus, for each value of L, the critical exponent $\gamma = 1$ follows from (1.5) or (1.6) where the L-dependent connective constant is given by $\mu_L = 1/x_c(L)$. The L-dependent amplitude A_L is given in table 2.

2.2.3. Finite-size scaling. Here we look at the finite-size scaling of the peak in the analogue of the heat capacity. First, we make a trivial modification of definition (1.2) in order to define the quantity $V(x, L, M)$ for the $L \times M$ rectangle. Figure 4(*a*) illustrates the classic finite-size rounding with M of the critical-point divergence (see, e.g., [4]). In view of (1.4) we expect

$$x_m(M) - x_c(L) \sim M^{-\lambda} \tag{2.10}$$

where $x_m(M)$ is the location of the peak for finite M and the critical points $x_c(L)$ are as given in table 2. By numerically calculating $x_m(M)$ for a sequence of M values at given L, we find the exponent appearing in (2.10) is consistent with the value $\lambda = 1/\nu = 2$ (see figure 4(*b*)).

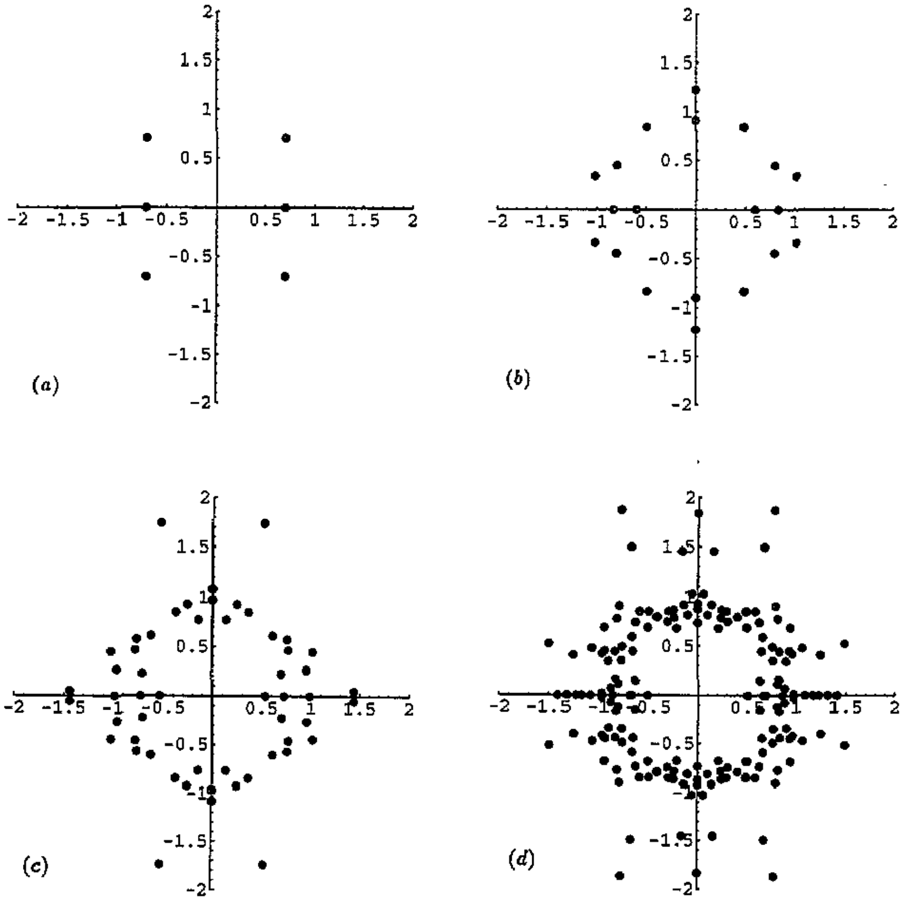

Figure 3. All poles of the generating function $C_{L,\infty}$ for (*a*) $L = 2$, (*b*) $L = 3$, (*c*) $L = 4$, and (*d*) $L = 5$.

Table 2. Values with increasing strip width L of (i) the dominant pole $x_c(L)$ in the generating functions $C_{L,\infty}(x)$ and $P_{L,\infty}(x)$, (ii) the amplitude A_L appearing in (2.9), and (iii) the exponent estimate λ_L of (4.1).

L	$x_c(L)$	A_L	λ_L
1	1.000 000	−1.000 000	
2	0.707 107	−0.300 000	0.92
3	0.594 616	−0.124 655	1.04
4	0.536 749	−0.062 381	1.09
5	0.501 896	−0.035 011	1.12
6	0.478 782		1.14
7	0.462 427		1.16
∞	0.379 052		

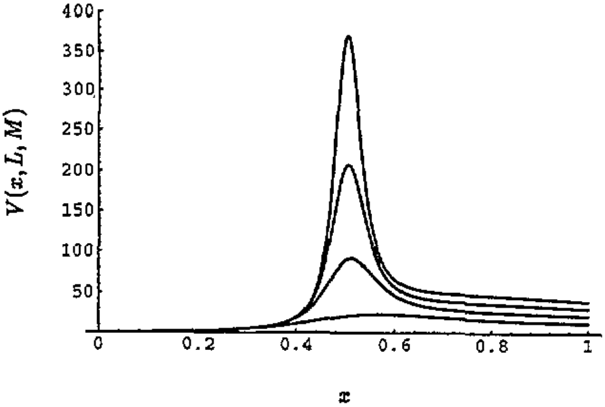

(a)

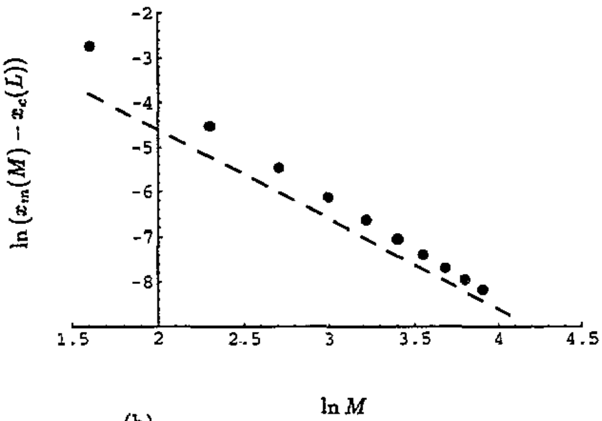

(b)

Figure 4. (*a*) Peaks in the analogue of the heat capacity $V(x, L, M)$ as a function of x for $L = 5$. Successively higher peaks correspond to the values $M = 5, 10, 15, 20$. The curves for $M = 5$ and $M = 10$ follow from the data given in table 1. (*b*) The corresponding test of the finite-size scaling of the peaks in $V(x, L, M)$ for $L = 5$ and $M = 5, 10, 15, \ldots, 50$. The broken line has a gradient of -2.

2.3. Generating functions for the full strip

The self-avoiding walks from the SW to the SE corner of the infinitely high rectangle are essentially walks confined to a half-strip. Here we consider self-avoiding walks across a full strip, as depicted in figure 5. For such walks, we introduce a further transfer matrix $\mathbf{S}$ to incorporate the initial and final steps of the walk. The corresponding arrow configurations represent a source and a sink. The six allowed vertices and their corresponding weights are given in figure 6. In this case, the factors of i and $-$i have been chosen to ensure that the correct weight is given to each of the nine possible combinations of the initial and final arrow configurations. This is the analogue of the factor $-ix$ appearing in the denominator of (2.3). Indeed, a similar source–sink matrix could have been introduced for the corresponding walk in the half-strip.

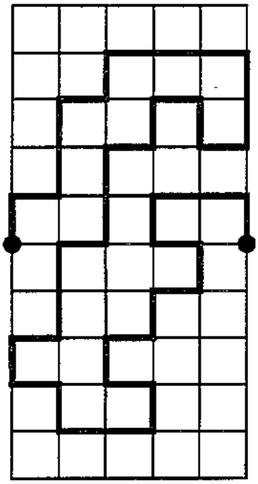

Figure 5. A typical self-avoiding walk across the full strip.

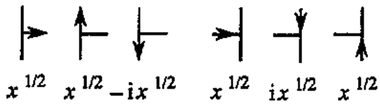

Figure 6. The boundary-source and -sink arrow configurations and corresponding vertex weights for the transfer matrix **S** for self-avoiding walks across the full strip.

In this case, consider an $L \times 2M$ rectangle, then the generating function can be written

$$C_{L,M}(x) = \langle\psi|\mathbf{T}^M\mathbf{S}\mathbf{T}^M|\psi\rangle \tag{2.11}$$

where $\psi = |||\cdots|||$ is the null state. We find that the generating function for the infinite strip is of the form

$$C_{L,\infty}(x) = \frac{\bar{p}_L(x)}{[q_L(x)]^2} \tag{2.12}$$

where $q_L(x)$ is the *same* function that appears for the half-strip. Thus, the same simple poles now appear as double poles. The first few $\bar{p}_L(x)$ are

$$\begin{aligned}
\bar{p}_1(x) &= 2x \\
\bar{p}_2(x) &= y(1+2y-6y^2+2y^3-7y^4-2y^6) \\
\bar{p}_3(x) &= xy(1+y)(1+3y-35y^2+53y^3+48y^4-158y^5+74y^6+66y^7-56y^8+32y^9-112y^{10} \\
&\quad +114y^{11}+33y^{12}-141y^{13}+51y^{14}+55y^{15}-48y^{16}+20y^{17}+16y^{18}-8y^{19}).
\end{aligned} \tag{2.13}$$

The appearance of the double poles is reflected in the recurrence relations for the series coefficients, where they appear as double roots in the characteristic equation. The generating function behaves as

$$C_{L,\infty}(x) \sim B_L(x-x_c(L))^{-2}. \tag{2.14}$$

Thus, through (1.5), we have the exponent $\gamma = 2$ for self-avoiding walks across the full strip.

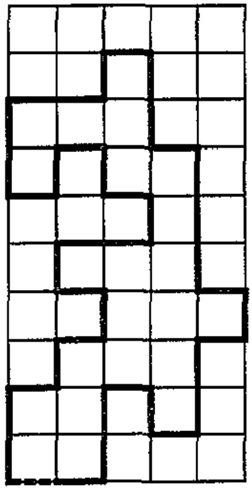

Figure 7. A typical self-avoiding polygon rooted to the SW corner of the half-strip. Each allowed n-sided polygon must have the indicated broken line as part of its perimeter.

3. Self-avoiding polygons

In this section, we return to the half-strip and consider the matrix element

$$P_{L,M}(x) = \mathrm{i}\langle\phi|\mathsf{T}^m|\psi\rangle - x^2 \tag{3.1}$$

with the initial and final states $\phi = \uparrow\downarrow|\cdots\|\,|$ and $\psi = |\,\|\cdots\|\,|$. This is the generating function for self-avoiding polygons rooted at the SW corner of an $L \times M$ rectangle (see figure 7). In this case, we find

$$P_{L,\infty}(x) \doteq \frac{\hat{p}_L(x)}{q_L(x)} \tag{3.2}$$

where $q_L(x)$ is again as given in (2.5). Thus, the series coefficients obey the same recurrence relations (2.7) and so the critical behaviour is seen to be indentical to that of the self-avoiding walk problem across the half-strip—which is not surprising given that the difference between the two problems lies essentially in the choice of matrix element. The explicit difference appears in the numerator, with

$$\begin{aligned}
\hat{p}_1(x) &= y^2 \\
\hat{p}_2(x) &= y^2(1+2y^2) \\
\hat{p}_3(x) &= y^2(1-2y+y^2+3y^3-y^4-3y^5-6y^6+5y^7-4y^9) \\
\hat{p}_4(x) &= y^2(1-4y+2y^2+12y^3-15y^4+3y^5+41y^6-111y^7+3y^8+151y^9-173y^{10}-217y^{11} \\
&\quad +455y^{12}+10y^{13}-617y^{14}+431y^{15}+441y^{16}-721y^{17}+23y^{18}+738y^{19} \\
&\quad -447y^{20}-189y^{21}+314y^{22}-64y^{23}-39y^{24}+4y^{25}+4y^{26}).
\end{aligned} \tag{3.3}$$

The generating function (3.2) thus behaves as

$$P_{L,\infty}(x) \sim C_L(x - x_c(L))^{-1}. \tag{3.4}$$

4. Discussion

In this paper, we have algebraically constructed the exact generating function of a number of self-avoiding-walk problems confined to infinitely long strips of finite width. Our key point is the use of exact transfer-matrix enumeration with the aid of MATHEMATICA. This approach is limited by the increasing size of the transfer matrix. However, beyond working with only the relevant sector of the transfer matrix, we have made no attempt to reduce the matrix size by use of symmetries etc. Thus, larger widths could be treated in principle, although the sheer length of the series and the size of the coefficients could be a limiting factor in constructing the exact generating function via Padé approximants. On the other hand, one could employ, in a similar way, the original two-state transfer matrix of Klein [9] which is considerably smaller in size.

Our chief finding is that the generating functions for the infinite strips are simply ratios of polynomials with either simple poles, in the case of the half-strip, or double poles for the full strip. In this way, we do not see the bulk exponent $\gamma = \frac{43}{32}$ but rather $\gamma = 1$ and $\gamma = 2$. For large but finite L we still expect to see these same exponents. Only in the thermodynamic $L \to \infty$ limit will we recover the true bulk critical behaviour, where the pole structure indicated in figure 3 for finite L must develop a branch cut responsible for the non-integer exponent. The vanishing of the amplitude A_L with increasing L in the dominant simple pole structure of (2.9) is consistent with this picture (see table 2). We also see the finite-size scaling exponent $\nu = \frac{1}{2}$ rather than $\nu = \frac{3}{4}$. Similar behaviour occurs in the finite-size scaling of the Ising model. In the present case, this is due to the inherent one-dimensional or Gaussian nature of self-avoiding walks in strips [9].

One remaining question concerns how the values $x_c(L)$ approach the bulk value x_c with increasing L. Here, an analogue is a stack of L isotropically interacting planar Ising models, where one seeks to quantify the finite-size scaling of the L-dependent critical temperature towards the bulk three-dimensional value. This is still an open question. Assuming an L-dependence, as in (1.4), with exponent $-\lambda$ and adopting the successive two-point estimators λ_L defined by (see also [16, 9])

$$\lambda_L = \frac{\ln(\phi_{L-1}/\phi_L)}{\ln(L/(L-1))} \qquad \text{where } \phi_L = x_c(L) - x_c \tag{4.1}$$

leads to the series of estimates shown in table 2. Thus, the exact value $\lambda = 1/\nu = \frac{4}{3}$ appears likely.

Acknowledgments

It is a pleasure to thank M N Barber for a number of helpful comments. This work has been supported by the Australian Research Council.

Appendix

Here we give the exact generating function $C_{5,\infty}(x)$ for which the polynomials defined in (2.4) are

$$p_5(x) = xy^2(1+y)(1+5y-39y^2-80y^3+495y^4+637y^5-3569y^6-3014y^7+17\,692y^8$$

$$+7752y^9-64\,969y^{10}-2649y^{11}+181\,409y^{12}-62\,246y^{13}-386\,507y^{14}$$
$$+298\,730y^{15}+589\,586y^{16}-839\,140y^{17}-480\,971y^{18}+1\,640\,953y^{19}$$
$$-389\,805y^{20}-2\,232\,360y^{21}+2\,196\,899y^{22}+1\,838\,658y^{23}-4\,377\,935y^{24}$$
$$-86\,028y^{25}+5\,688\,958y^{26}-2\,168\,282y^{27}-5\,516\,611y^{28}+3\,818\,810y^{29}$$
$$+3\,714\,749y^{30}-3\,944\,164y^{31}+1\,363\,348y^{32}-2\,675\,454y^{33}-4\,562\,534y^{34}$$
$$+16\,158\,379y^{35}-3\,681\,898y^{36}-21\,631\,824y^{37}+14\,798\,711y^{38}$$
$$+11\,176\,389y^{39}-7\,363\,740y^{40}-4\,685\,687y^{41}-14\,921\,354y^{42}$$
$$+27\,402\,763y^{43}+4\,888\,070y^{44}-37\,118\,551y^{45}+32\,376\,683y^{46}$$
$$-16\,062\,195y^{47}-2\,598\,866y^{48}+33\,868\,689y^{49}-5\,460\,9387y^{50}$$
$$+37\,756\,383y^{51}+390\,287y^{52}-28\,963\,676y^{53}+40\,473\,783y^{54}$$
$$-34\,066\,023y^{55}+10\,898\,031y^{56}+14\,119\,932y^{57}-2\,2534\,942y^{58}$$
$$+12\,496\,434y^{59}+1\,901\,822y^{60}-9\,902\,644y^{61}+10\,652\,313y^{62}-7\,494\,907y^{63}$$
$$+3\,691\,576y^{64}-1\,105\,899y^{65}+424\,52y^{66}+211\,571y^{67}-265\,241y^{68}$$
$$+233\,452y^{69}-124\,866y^{70}+31\,978y^{71}+797y^{72}-2982y^{73}+974y^{74}-200y^{75}$$
$$+12y^{76}+8y^{77}) \tag{A.1}$$

$$q_5(x)=1-9y+16y^2+71y^3-232y^4-288y^5+1593y^6+350y^7-7014y^8+3348y^9$$
$$+20\,239y^{10}-22\,003y^{11}-42\,092y^{12}+78\,021y^{13}+62\,058y^{14}$$
$$-190\,408y^{15}-61\,536y^{16}+341\,452y^{17}+71\,641y^{18}-511\,606y^{19}-511\,606y^{19}$$
$$-239\,641y^{20}+838\,413y^{21}+668\,471y^{22}-1\,732\,194y^{23}-949\,258y^{24}$$
$$+3\,819\,977y^{25}-545\,529y^{26}-6\,513\,308y^{27}+5\,397\,238y^{28}+7\,199\,583y^{29}$$
$$-12\,880\,746y^{30}-4\,621\,472y^{31}+23\,215\,130y^{32}-3\,380\,541y^{33}-32\,687\,193y^{34}$$
$$+16\,206\,393y^{35}+34\,622\,073y^{36}-27\,262\,271y^{37}-25\,981\,314y^{38}$$
$$+23\,521\,540y^{39}+8\,593\,823y^{40}+16\,676\,694y^{41}-19\,203\,008y^{42}$$
$$-61\,047\,969y^{43}+65\,229\,299y^{44}+60\,155\,517y^{45}-87\,205\,992y^{46}$$
$$-31\,219\,707y^{47}+49\,239\,535y^{48}+38\,596\,642y^{49}-11\,814\,375y^{50}$$
$$-90\,930\,608y^{51}+54\,774\,818y^{52}+84\,911\,801y^{53}-138\,005\,443y^{54}$$
$$+75\,414\,241y^{55}+28\,683\,931y^{56}-121\,545\,274y^{57}+169\,670\,616y^{58}$$
$$-144\,813\,943y^{59}+46\,944\,365y^{60}+81\,961\,838y^{61}-170\,841\,948y^{62}$$
$$+160\,982\,866y^{63}-68\,522\,458y^{64}-30\,418\,321y^{65}+75\,337\,881y^{66}$$
$$-62\,928\,205y^{67}+27\,960\,732y^{68}-1\,670\,870y^{69}-7\,168\,755y^{70}+5\,262\,460y^{71}$$
$$-1\,286\,784y^{72}-598\,456y^{73}+496\,076y^{74}-21\,034y^{75}-72\,348y^{76}$$
$$-1412y^{77}+18\,120y^{78}-2684y^{79}-1706y^{80}+300y^{81}+112y^{82}-8y^{83}-8y^{84}. \tag{A.2}$$

References

[1] Whittington S G and Guttmann A J 1990 *J. Phys. A: Math. Gen.* **23** 5601
[2] Burkhardt T W and Guim I 1991 *J. Phys. A: Math. Gen.* **24** L1221
[3] Prentis J J 1991 *J. Phys. A: Math. Gen.* **24** 5097
[4] Barber M N 1983 *Phase Transitions and Critical Phenomena* vol 8, ed C Domb and J L Lebowitz (London: Academic) p 145
[5] Guttmann A J and Enting I 1988 *J. Phys. A: Math. Gen.* **21** L165
[6] Nienhuis B 1982 *Phys. Rev. Lett.* **49** 1062
[7] Batchelor M T 1994 *Phys. Lett.* **184A** 467
[8] Wall F T, Seitz W A and Chin J C 1977 *J. Chem. Phys.* **67** 434
[9] Klein D J 1980 *J. Stat. Phys.* **23** 561
[10] Batchelor M T and Suzuki J 1993 *J. Phys. A: Math. Gen.* **26** L729
[11] Derrida B 1981 *J. Phys. A: Math. Gen.* **14** L5
[12] Enting I 1980 *J. Phys. A: Math. Gen.* **13** 3713
[13] Domany E, Mukamel D, Nienhuis B and Schwimmer A 1981 *Nucl. Phys.* B **190** 279
[14] Nienhuis B 1990 *Int. J. Mod. Phys.* B **4** 929
[15] de Gennes P G 1972 *Phys. Lett.* **38A** 339
[16] Guttmann A J and Whittington S G 1978 *J. Phys. A: Math. Gen.* **5** L107